Changes in grain size distribution and topography of mountainous river bed by landslide dam failure

Akihito KAJI[1,*] Takeshi SHIMIZU[2], Taro UCHIDA[3], Tadanori ISHIZUKA[2], Koji MORITA[2], Yuki OKUYAMA[3] and Satoshi NIWA[3]

[1] Public Works Research Institute (present (affiliation is/in) TOKEN C.E.E Consultants Co., Ltd.), 1-8-63 Tenmabashi Kitaku, Osaka, Osaka 5300042, Japan

[2] Volcano and debris flow research team, Erosion and Sediment Control Research Group, Public Works Research Institute, 1-6 Minamihara, Tsukuba, Ibaraki 3058516, Japan

[3] Erosion and Sediment Control Division, Research Center for Disaster Management, National Institute for Land and Infrastructure Management, 1 Asahi, Tsukuba, Ibaraki 3050804, Japan

*Corresponding author. E-mail: kaji-a@tokencon.co.jp

Landslide dams were formed as a result of the Iwate-Miyagi Nairiku earthquake in the Tohoku region, Japan, in July 2008. This study examines a landslide dam with height and width each approximately 50 m that failed by overtopping during Typhoon Jelawat on October 1, 2012. The debris flow shifted downward, and sediment was deposited from the landslide dam to a check dam located approximately 1.7 km downstream from the dam. Grain size distribution of the deposited sediment and topographical changes before and after the landslide dam failure are reported. For analysis of the change in grain size distribution at locations in which the depositional process was dominant, the area below the landslide dam was divided into three regions: downstream, middle stream, and upstream. The grain size distribution was greater in the downstream area than that of the upstream and middle stream area. The changes in longitudinal and cross-sectional profiles showed the same trends as those reported in previous researches.

Keywords: landslide dam, debris flow, grain size distribution, overtopping erosion

1. INTRODUCTION

When a massive landslide occurs on a hillside slope, sediments can be deposited in a river channel. Massive sediments deposition that causes complete or partial river blockage is known as a landslide dam. If the water level in a lake formed upstream of the landslide dam becomes higher than the height of the dam, the water flow begins to erode the massive sediment. If the sediment is rapidly eroded by the overflow in a process known as landslide dam overtopping, the debris flow can cause substantial damage to downstream areas. Overtopping is a main cause of the landslide dam failure [e.g., *Costa and Shuster*, 1988; *Tabata et al*., 2002]. Previous research includes various approaches used to determine the nature of landslide dams. For example, the relationship between geomorphic evidence and detailed analysis of historic documents has revealed occurrence characteristics of past large disasters [*Dai et al*., 2005; *Inoue et al*., 2008]. *Costa and Shuster* [1988], *Ishikawa et al.* [1992], *Casagli et al.* [2003], and *Korup* [2004] collected data on landslide dams occurring worldwide and compared the results with those occurring in their local regions. Hey proposed empirical relationships between the height and width of landslide dams and peak discharge upon erosion due to overtopping. An additional approach for investigating the physical process of overtopping during landslide dam failure is the use of laboratory experimental studies [*Oda et al*., 2006, 2007; *Cao et al*., 2011]. Many such studies focus on the nature of landslide dam overtopping or the shape of the landslide dam and upstream catchment. However, in studies of debris flow caused by overtopping, it is also important to investigate the state of the area downstream from the dam. *Casagli et al.* [2003] and *Wang et al.* [2012] reported that grain size distribution exerts control on dam stability, influencing the strength and the permeability of the dam material. Casagli et al. [2003] reported different grain size distributions

from data obtained from 42 landslide dams formed in Italy. Wang et al. [2012] examined the relationship between grain size distribution and current conditions of the remaining landslide dams formed after the Great Sichuan Earthquake of 2008, reporting a larger proportion of coarse gravels than failed landslide dams.

For a landslide dam formed by the Iwate–Miyagi Nairiku Earthquake in Japan in 2008, *Uchida et al.* [2009] reported the grain size distribution and the change in topography after the dam failed by overtopping. In this research, which was based on measuring by field survey, the erosion width ranged from 19 m to 32 m, the river bank slope ranged from 30° to 52°, and the longitudinal river bed gradient ranged from 2.4° to 7.5°. Regarding grain size distribution, the river bed material present at the location of the spillway created by overflow was found to be coarser than the landslide dam sediments. *Yoshino et al.* [2010] reported detailed topographical changes in the same landslide by using airborne LiDAR. They concluded that the width of the spillway created by overflow was wider and the erosional depth was smaller at the downstream area than that of the upstream. In addition, they reported that the longitudinal gradient of depositional area downstream from the dam had a gentler spillway gradient than that downstream.

For disaster prevention, it is important to investigate the stability of the landslide dam in addition to the debris flow properties after overtopping. Only a few reports [e.g., *Zhow et al.*, 2012] have presented field grain size distribution of both the landslide dam and the erosional and depositional areas by debris flow caused by landslide dam failure. The purpose of this paper is to investigate different studies of landslide dam failure in the Tohoku region reported by *Uchida et al.* [2009] and *Yoshino et al.* [2010], to examine the grain size distributions in the landslide dam body and downstream region, and to evaluate the details of topographic change.

2. STUDY AREA

The studied landslide dam in the Tohoku region in Japan (**Fig. 1**) was formed after collapse of a hillside during a June 2008 earthquake. The basin area of the landslide dam is approximately 17 km^2, the width of the river channel blockage is approximately 50 m, and the change in elevation between the original river bed and the dam crest is also approximately 50 m. These values are based on airborne LiDAR, which is described subsequently.

Immediately after its formation in July 2008, the landslide-dammed lake exceeded its full capacity, causing small-scale erosion due to overtopping.

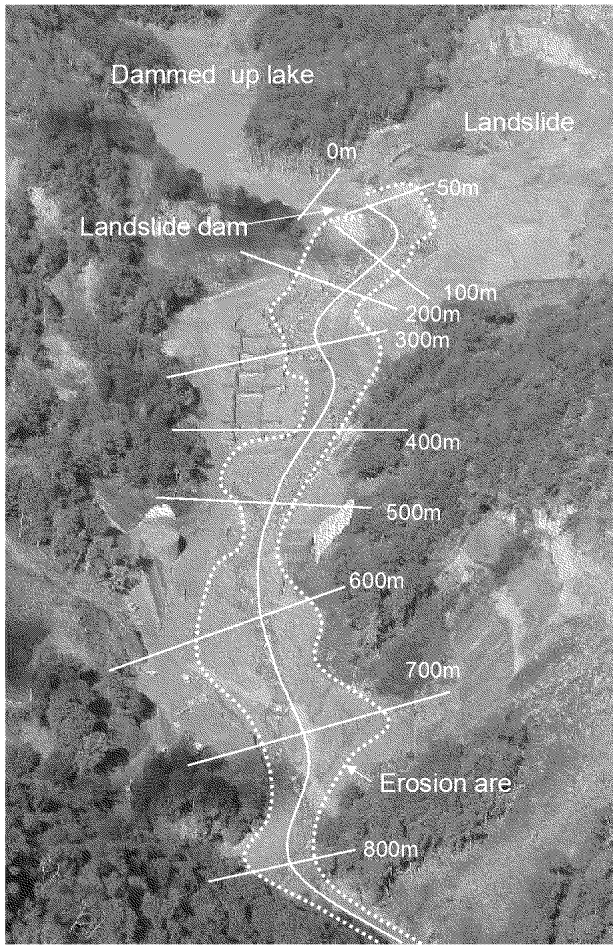

Fig. 1 study area (October 5.2012)

Although water flowed continuously over the landslide dam crest, the dam did not collapse because of channel and ground sill construction, which was performed just prior to the overtopping. Rather, rainfall from Typhoon Jelawat on October 1, 2012, resulted in overtopping. From September 30 to October 1, the total rainfall was 170 mm, and hourly rainfall was 57 mm, as recorded by the rain-gauge station located approximately 7 km east of the target area. Additionally a cell-type steel erosion control dam was under construction 500 m downstream of the dam, and a check dam had been constructed 1700 m downstream.

3. METHOD OF SURVEY

3.1 Survey of river bed materials

3.1.1 Grain size distribution

(1) Survey location

Six survey locations that were not affected by activity such as bulldozer action were selected to investigate changes in grain size distribution in both the landslide dam and the downstream area of the dam where the sediment of the debris flow was eroded and deposited (**Fig. 2**). These locations are listed below:

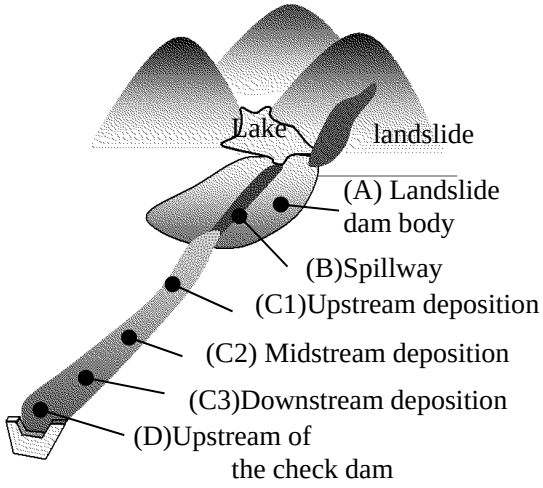

Fig. 2 schematic diagram of survey location

- (A) Landslide dam body
- (B) Spillway
- (C1) Upstream deposition
- (C2) Midstream deposition
- (C3) Downstream deposition
- (D) Upstream of the check dam

The dominant process of (A)–(B) was erosion, and that of (C)–(D) was deposition. The landslide dam body itself (A) is at the side bank of the river created by dam erosion. The erosional area (B) includes the river and a small terrace in the eroded landslide dam body. In this area, rocks exceeding 1 m in diameter exist. (C1), (C2), and (C3) were chosen to investigate the differences in grain size distribution in the deposition areas at greater distances. Upstream of the check dam (D) was selected to examine fine sediment distribution.

(2) Survey method

As reported by *Casagli et al.* [2003], it is important to measure coarse grains and fine sediment of a landslide dam. According to *Kawamura et al.* [1970], several survey methods are used to examine coarse grain size distribution in river beds. These approaches include area grid, line grid, surface sampling, and photographic methods. The area grid and surface sampling methods, which require survey ranges of several square meters, were not adopted because the widths of the erosion areas in (A) and (B) are several meters. The photographic measurement method, which measures two surface axes of grain, is less accurate than other methods that measure three axes of grain. Therefore, the line grid method was applied to measure grain size distribution.

The river bed field survey was conducted on October 12–13, 2012, 10 days after the overtopping occurred. For the line method, approximately 100 measuring points were set at grid intersections. The number of samples was determined to obtain statistically valid data [*Kawamura et al.*, 1970]. The specifications of the measuring points in each survey location are shown in **Table 1**. Among the six survey locations, the line grid method was conducted at five survey locations in which the river bed was covered with coarse grains: (A), (B), (C1), (C2), and (C3). Two adjacent upstream and downstream points were measured and considered as one location for (A) because the measurable area of the survey site is narrow and limited.

Table 1 list of points (Line Grid Method)

Location	Dam body	Spillway	Deposit	Deposit	Deposit
Section	—	—	UP	Mid	Down
Label	(A)	(B)	(C1)	(C2)	(C3)
Distance from Overtopping Point(m)	—	100	800	1100	1300
Number of Survey Line	2	4	4	4	4
Longitudinal Grid Interval(m)	2	2	2	2	2
Crossing Grid Interval (m)	1	2	2	2	2
MAX Survey Distance (m)	54	60	40	60	48
measureing points	66	112	84	114	100

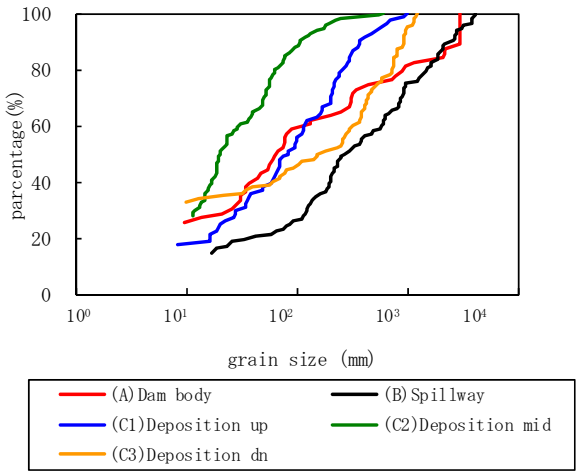

Fig. 3 grain size distribution

The procedure for obtaining grain size data at each measuring point is listed below:

- A grain present below the measuring point was picked up.
- Three axes (major, intermediate, and minor) were measured by using a ruler.
- The average length was calculated as data of that point.

It should be noted that grains smaller than or equal to 1 cm were recorded as 1cm.

3.1.2 Sediment concentration

(1) Survey location

To measure the volume sediment concentration of the deposited sediment, sediment was sampled at (C3) up to about 20 cm from the river channel edge. To compare the change in volume sediment concentration in the longitudinal direction of the river, the samples were collected from two points at

(A) and one point at (D).

(2) Survey method

The sampling was conducted from a nearly cubic-shaped hole dug at (C3) with an area of 50 cm^2 and a depth of 30 cm. Due to to onsite work restrictions, samples were collected manually by using a shovel. It should be noted that the volume reported is an approximation; the presence of gravels of several centimeters prohibited the formation of a flat surface for sampling.

The undisturbed sediment at (A) and (D) was collected by using a 100 ml soil sampling tube. The volume sediment concentration for each sample was determined by soil tests.

3.2 Topographic survey

3.2.1 Landform measurement before and after overtopping

The topographic information is based on 1 m mesh terrain elevation data measured by airborne LiDAR in November 2008 and October 2012, before and after overtopping erosion. On a shaded relief map created by using Geographic Information Systems (GIS) software, the center survey lines longitudinally between the erosion and deposition areas were drawn in order to obtain longitudinal profiles of the river bed at 1 m intervals. Next we drew a lateral sectional survey line perpendicular to and intersecting the longitudinal survey line at 100 m intervals from the overtopping point of the natural dam downstream to obtain lateral sectional profiles of the erosion and deposition areas.

3.2.2 Calculation of river bed elevation changes

By using the longitudinal profile, the changes in river bed elevation were calculated at 1 m intervals.

3.2.3 Calculation of longitudinal gradient

The longitudinal gradient was calculated at 200 m intervals to determine changes in the gradient.

4. SURVEY RESULTS

4.1 River bed survey

4.1.1 Grain size distribution

The grain size distribution at each grain size survey point is shown in **Fig. 3**. A comparison of grain size distributions at (A) and (B) revealed that the grain size at (B) was generally coarser than that at (A). Within all deposition sites, the distribution of grain sizes d_{100} and d_{50} at (C2) was less than that at (C1) and (C3). The percentage of grains at 1 cm in diameter was highest at (C3), and (C3) had a wider grain size range than (C1) and (C2). Greater amounts of gravel and rocks occurred at (C3) in comparison with those at (C1) and (C2).

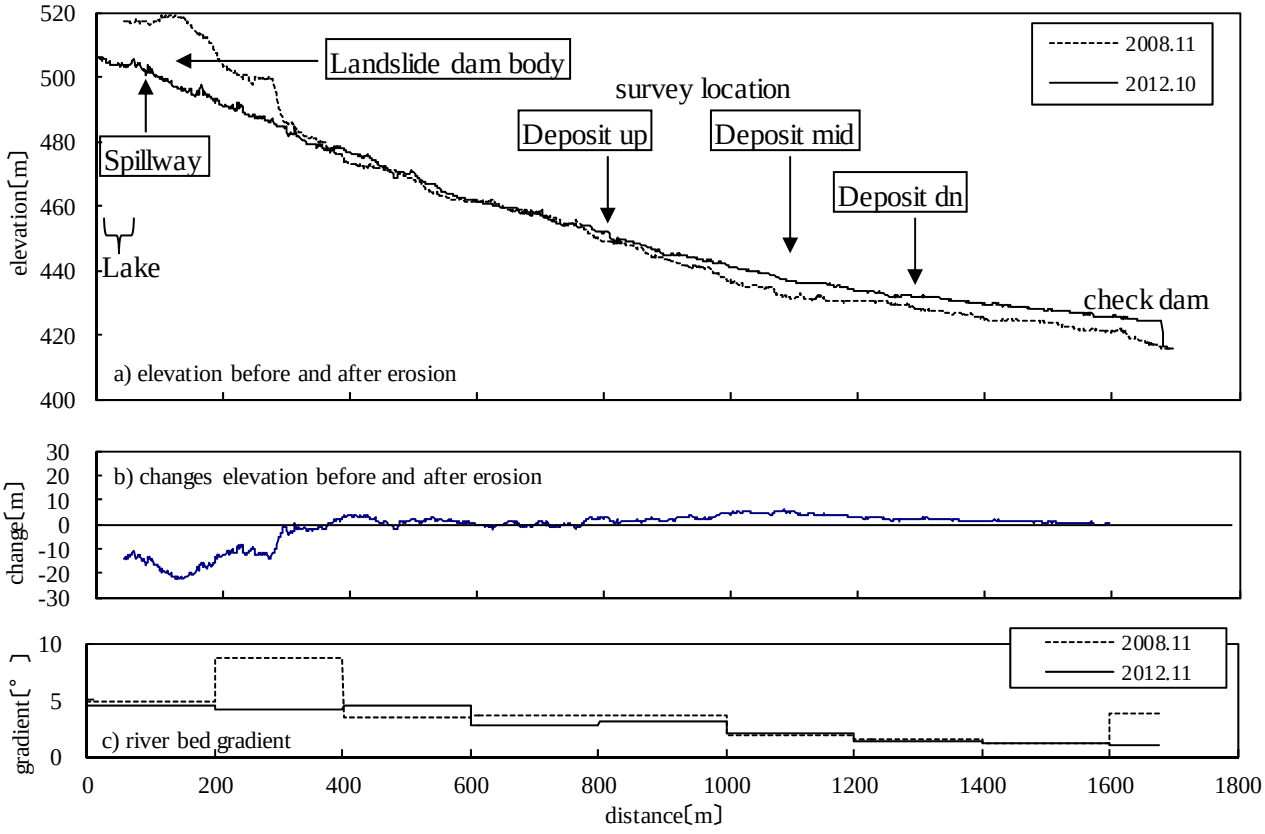

Fig. 4 LiDAR longitudinal profile

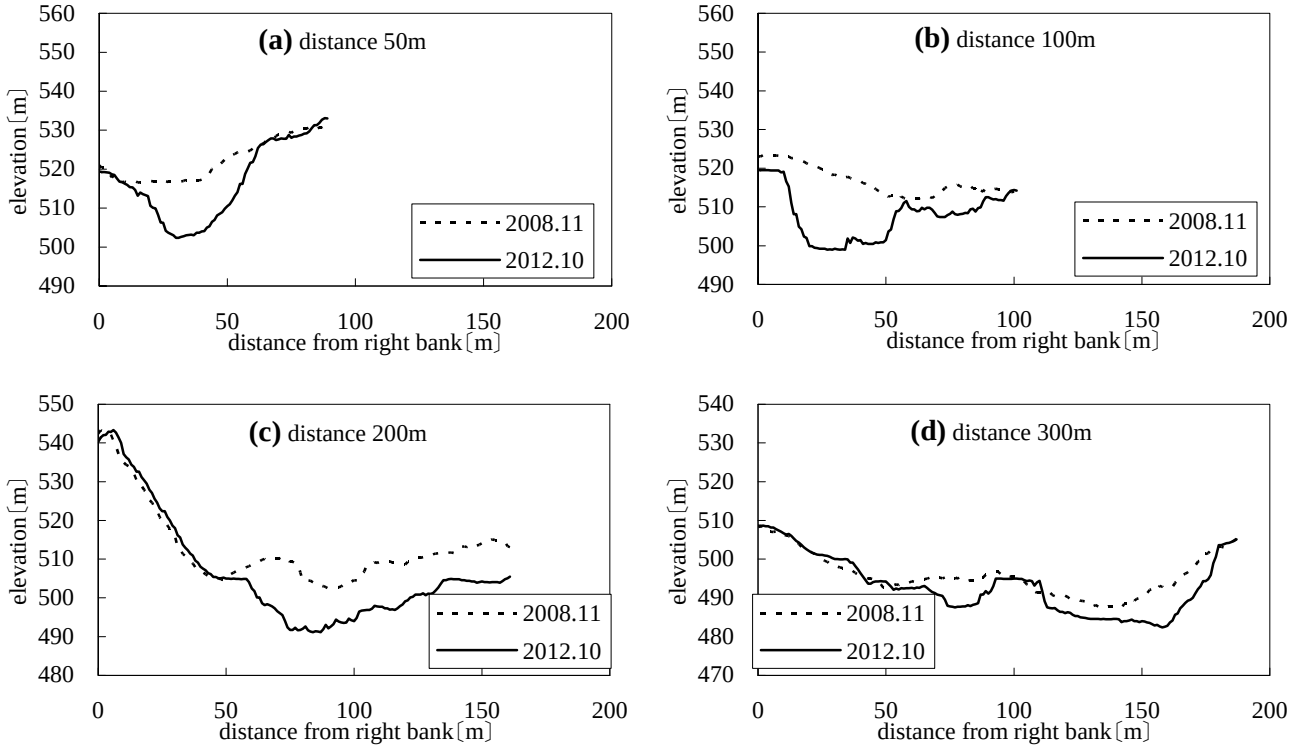

Fig. 5 Cross sectional profile of erosion area

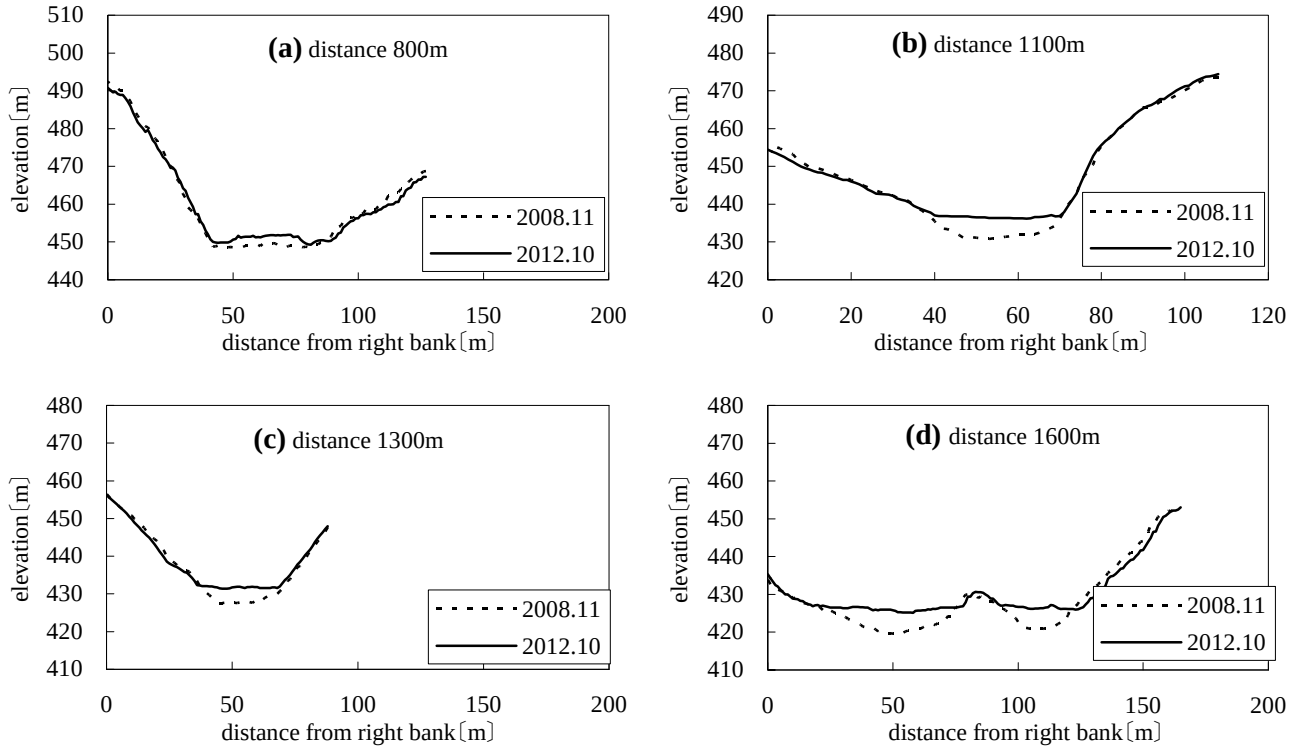

Fig. 6 Cross sectional profile of deposition area

4.1.2 Sediment concentration

The volume sediment concentration in the static river bed at (C3) was 0.464. This value is higher than that in the undisturbed sample taken from (D) and smaller than that taken from (A). The value of (D) was 0.448, and those of (A) were 0.486 and 0.536.

4.2 Topographical survey

4.2.1 Longitudinal profile

The LiDAR longitudinal profiles are shown in **Fig 4.** Image (a) shows the elevation before and after erosion, image (b) shows changes in the river bed elevation before and after erosion, and image

(c) shows the river bed gradient. The horizontal axis indicates the distance (m) downstream from the upstream border of the erosion area. It should be noted that the landslide dam was 0 m to 50 m from the lake prior to the overtopping erosion (November 2008); thus, this area was excluded from the comparison.

As shown in **Figs. 4 (a)** and **(b)**, the section in which the landslide dam body existed was eroded. The erosion length is approximately 350 m, and the maximum erosion depth is approximately 23 m (at a distance of 140 m). Sediment was deposited from a distance of 350–1700 m. The check dam at 1700 m is located at the edge of the debris flow. The maximum deposition height is approximately 6 m at a distance of 1100 m.

Fig. 4 (c) shows that the longitudinal gradient before erosion (November 2008) was 3.3°–3.5° at a distance of 400–1000 m and 1.1°–1.8° at 1000–1600 m. After erosion (October 2012), the longitudinal gradients were 2.7°–4.4° and 1.1°–2.1° at the same distances, respectively. Thus, little gradient change appeared after the overtopping. The gradient of the landslide dam body changed to match the longitudinal gradient of the downstream deposition area after erosion.

4.2.2 Cross-sectional profile

The selected cross-sectional profiles are shown in the erosional area in **Fig. 5** and the depositional area in **Fig. 6** as viewed from the downstream side.

The erosion depth of the curved part at **Fig. 5 (a)** is approximately 14 m. To compare the change in erosion width, which is the value calculated at the flat part of the cross-sectional profile near the bottom in October 2012, the value of **Figs. 5 (a)** to **(d)** are indicated as follows. The changes are approximately 16 m in **Fig. 5 (a)**, approximately 28 m in **Fig. 5 (b)**, approximately 29 m **(**unclear bottom shape) in **Fig. 5 (c)**, and approximately 62 m in **Fig. 5 (d)**. These data indicate that the erosion width was greater downstream.

The river bank gradient is approximately 46° on the right bank and approximately 47° on the left bank, as shown in **Fig. 5 (a)**. The steepest slope is approximately 58° on the right bank shown in **Figs. 5 (b)** and **(d)**, and the gentlest slope is approximately 14° on the left bank shown in **Fig. 5 (c)**. In the field survey, an area assumed to be natural ground was observed on the left bank shown in **Fig. 5 (a)**, although the other stream bank in the erosion area formed the landslide dam.

Conversely, in the deposition area shown in **Figs. 6 (a)** to **(d)**, magnification of the river width and river bank gradient could not be identified.

5. DISCUSSION

5.1 Changes in grain size distribution

Ideally, the grain size at (C3) was considered to be finer because the river bed gradient is gentler than that at (C1) upstream. Thus, the tractive force is lower at (C3) than (C1).

On the basis of grain size distributions at (C1)–(C3) shown in **Fig. 3**, however, our grain size survey revealed that the grain size at (C3) was coarser than that at (C1) and (C2). This result occurred because (C3) is located at the debris flow front at the longitudinal concave line.

According to *Zhou et al*. [2012], the grain size in the debris flow front gradually coarsened as it flowed downstream. After the debris flow front passed, the river bed grain was refined as the discharge was reduced. In this study, (C3) exhibited a high percentage of grains with diameters of 1 cm or less, and the grain size distribution extended over a wide range because the debris flow with peak discharge carried coarser gains. Moreover, the subsequent flow with smaller discharge carried finer gains in the area after the debris flow front stopped.

5.2 Estimation of topography just prior to overtopping

The check dam was constructed after the landslide dam formed, but small-scale overflow overtopping occurred and water flowed continuously over the landslide dam crest. By the field survey, sediments were deposited on the river bed of the left side stream upstream of the check dam and as high as the spillway elevation of the check dam. In addition, a landslide provided sediments upstream of the side stream. Based on these facts, it was estimated sediment deposition was in progress upstream of the dam after construction of the check dam.

We accordingly estimated the river bed elevation with sediments deposited upstream of the check dam as the longitudinal profile in September 2012, i.e., before the overtopping erosion occurred in October 2012.

In comparison with LiDAR shown in **Fig. 4 (a)** for the upstream side of the check dam, the actual elevation of the river bed prior to the overtopping could be estimated to be higher. The topography of the river bed was estimated in previous research [*Endo*, 1958] by using half the river bed gradient before the deposition elevation. That is, half of the gradient of 1.5° calculated 600 m upstream from the check dam was measured at 2008.11 by using LiDAR. Thus, the river bed from 1100 m to 1700 m was estimated as shown in **Fig. 7**.

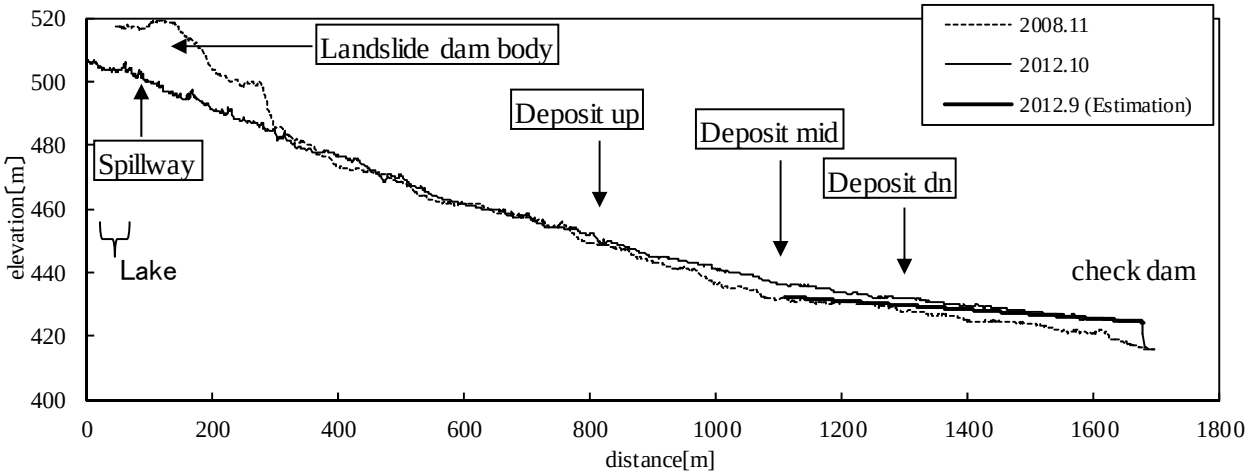

Fig. 7 Estimated riverbed longitudinal profile

5.3 Topographical changes in the cross-sectional direction

As shown in the cross-sectional profile in **Fig. 5**, the river bank gradient of the left and right banks in the erosion area is 14°–58°, although *Uchida et al.* [2009] reported gradients of 30°–52° at the erosion area in a different landslide dam. Both surveys showed that the steepest gradient exceeded 50°, which is larger than the general angle of repose of sand. In addition, the bottom of the erosion area widened downstream.

5.4 Estimation of peak discharge and velocity

The discharge was estimated by using Manning formula:

$$Q = A \cdot \frac{i^{1/2} \cdot R^{2/3}}{n}, \qquad (1)$$

where A is the cross-section area, n is the roughness coefficient, i is the gradient of the river bed, and R is the hydraulic radius. On the basis of field survey, the hydraulic radius was estimated by flood marks observed 4 m above the spillway of the check dam, and the spillway width was estimated as 18 m. The roughness coefficient used was 0.1, which is roughness in mountainous river beds, according to the Manual of Technical Standard for establishing Sabo master plan for debris flow and driftwood [*MLIT*, 2007]. The river bed gradient used was 0.8°, which was estimated as the upstream gradient in September 2012, as shown in **Fig. 4**. Thus, the discharge was calculated as 168 m^3/s, and the average velocity was 2.3 m/s. However, these values are believed to be underestimated. Although the values were estimated according to flood marks on the check dam, the inflows from the left side tributary located upstream of the check dam were not considered. For this reason, the differences between their peak time and the peak debris flow discharge from the collapse of the overtopped landslide dam were unknown. Additionally, the water level gauge installed near the crest of the landslide dam unfortunately was not operational during the typhoon, and a different water level gauge downstream of the check dam was under the effects of other tributaries.

The distances of 800 m and 1100 m shown in **Figs. 6 (a)** and **(b)** represent the right and left outer banks of the bend section. The section after deposition shows that the height did not increase relative to the inner bank. No significant drift was observed in the field survey, as determined by lodging or flattening of plants rooted on the side bank. In addition, no significant damage to the dam under construction at 500 m away was observed. We determined that the flow depth and velocity of the debris flow were not large enough to cause drift to destroy structures.

6. CONCLUSION

The results of the grain size distribution and topographical surveys of the landslide dam failure are revealed in the following points:

(a) The erosion length of the landslide dam is approximately 350 m, and the maximum erosion depth is approximately 23 m. The erosion width is 28–62 m (bottom width), which widened downstream. The side bank gradient in the erosion area is 14°–58°. The erosion width in the downstream spillway is larger, which is in good agreement with that reported by *Yoshino et al.* [2010].

(b) Deposition occurred in a section approximately 1350 m up to the check dam. The maximum deposition height calculated from the LiDAR difference is approximately 6 m.

(c) The longitudinal gradient both before and after

the overtopping was 3°–4° from the lower end of the landslide dam body to a distance of 1000 m and 1°–2° farther downstream. After overtopping, the gradient in the landslide dam body longitudinal profile changed, which is similar to that noted in the downstream section.

(d) The sediment was deposited just downstream of the landslide dam. Moreover, the longitudinal gradient of the depositional area was gentler than the downstream slope of the landslide dam. These trends are in good agreement with that reported by *Yoshino et al*. [2010].

(e) A comparison of grain size distribution in the landslide dam body and the erosion area revealed that grain coarsening occurred. Coarsening by landslide dam overtopping was also reported by *Uchida et al*. [2009].

(f) The distribution of grain sizes d_{100} and d_{50} in the deposit area are largest in the downstream area, which also has the highest percentage of 1 cm grain sizes. The grain size distribution range of the downstream area is broader compared with that in the upstream and middle stream in the deposition area.

(g) The volume sediment concentration in the deposited sediment was measured to be 0.464.

(h) The peak discharge was estimated on the basis of the flood marks on the check dam most downstream of the deposit area.

(i) On the basis of the cross-sectional profile after deposition and the flood marks on the left and right banks, the debris flow caused by the overtopping erosion was not sufficient in flow depth and velocity to damage the structures.

ACKNOWLEDGMENTS

The airborne LiDAR measured in November 2008 and October 2012 was supplied by the Kitakamigawa-karyu River Office, Tohoku Regional Development Bureau, Ministry of Land, Infrastructure, Transport and Tourism, Japan.

REFERENCES

Cao, Z., Yue, Z. and Pender, G. (2011): Landslide dam failure and flood hydraulics. Part I: experimental investigation, Natural Hazards, Vol.59, pp.1003–1019.

Casagli, N., Ermini, L. and Rosati, G. (2003): Determining grain size distribution of material composing landslide dams in the Northern Apennine: sampling and processing methods, Engineering Geology, Vol.69, pp.83-97.

Costa, J.E. and Schuster, R.L. (1988): The formation and failure of natural dams, Geological Society of American Bulletin, Vol.100, pp.1054-1068.

Dai, F.C., Lee, C.F., Deng, J.H., Tham, L.G. (2005): The 1786 earthquake - triggered landslide dam and subsequent dam - break flood on the Dadu River, southwestern China, Geomorphology, Vol.65, pp.205-221.

Endou, R. (1958): Erosion control engineering, Kyouritu Syuppan, pp.77 (in Japanese).

Inoue, K., Mori, T. and Mizuyama, T. (2008): Two large-scale landslide dams and outburst disaster in the Yoshino River, central Japan, Interpraevent2008, pp.188-189.

Ishikawa, Y., Irasawa, M. and Kuang, S.F. (1992):Study on prediction and countermeasures of flood disasters caused by landslide dam failures, Journal of Japan Society of Erosion Control Engineering, Vol.45, No.1, pp.14-21 (in Japanese).

Kawamura, S., Ozawa, K. (1970):Particle size distribution and sampling method of bed material in mountain rivers, Japan Society of Civil Engineers Journal, Vol.55, No.12, p.53-57 (in Japanese).

Korup, O. (2004): Geomorphometric characteristics of New Zealand landslide dams, Engineering Geology, Vol.73, p.13-35

National Institute for Land and infrastructure Management (2007): Manual of Technical standard for establishing sabo master plan for debris flow and driftwood, pp.32-53.

Oda, A., Mizuyama, T., Hasegawa, Y., Mori, T. and Kawada, K. (2006): Experimental study of process and outflow rate when landslide dams outburst, Journal of Japan Society of Erosion Control Engineering, Vol.59, No.1, pp.29-34 (in Japanese).

Oda, A., Mizuyama, T., Hasegawa, Y. (2007): An experiment on a landslide dam outburst, Journal of Japan Society of Erosion Control Engineering, Vol.60, No.2, pp.33-38 (in Japanese).

Tabata, S., Mizuyama, T. and Inoue, K. (2002): Landslide dams and Disasters, Kokon Syoin, pp.50-62 (in Japanese).

Uchida, T., Matsuoka, A., Matsumoto, N., Matsuda, J., Akiyama, K., Tamura, K. and Ichinohe, K. (2009): Overtopping erosion of landslide dam at Numakura-Urasawa, San-hazama river Miyagi Prefecture, Japan, Journal of the Japan Society of Erosion Control Engineering, Vol.62, No.3, pp.23-29 (in Japanese with English abstract).

Wang, Z., Cui, P., Yu, G. and Zhang, K. (2012): Stability of landslide dams and development of knickpoints, Environ Earth Science, Vol.65, pp.1067-1080

Yoshino, K., Uchida T., Tamura, K. and Kotake, T. (2010): Sediment transport of landslide dam by overtopping erosion: Analysis by LiDAR data, Journal of the Japan Society of Erosion Control Engineering, Vol. 62, No. 5, p. 27-35 (in Japanese with English abstract)

Zhou, G. G. D. Cui, P. Chen, H. Y. Zhu, X. H. Tang, J. B. and Sun, Q. C. (2012): Experimental study on cascading landslide dam failures by upstream flows, Landslides, Vol.10, p.633-643.